Published in final edited form as:
J Comp Neurol. 2011 December 15; 519(18): 3684–3699. doi:10.1002/cne.22681.

Subcellular Localization of Patched and Smoothened, the Receptors for Sonic Hedgehog Signaling, in the Hippocampal Neuron

Ronald S. Petralia[1], **Catherine M. Schwartz**[2], **Ya-Xian Wang**[1], **Mark P. Mattson**[2], and **Pamela J. Yao**[2,*]

[1]Laboratory of Neurochemistry, National Institute on Deafness and Other Communication Disorders, National Institutes of Health, Bethesda, Maryland 20892

[2]Laboratory of Neurosciences, National Institute on Aging Intramural Research Program, Baltimore, Maryland 21224

Abstract

Cumulative evidence suggests that, aside from patterning the embryonic neural tube, Sonic hedgehog (Shh) signaling plays important roles in the mature nervous system. In this study, we investigate the expression and localization of the Shh signaling receptors, Patched (Ptch) and Smoothened (Smo), in the hippocampal neurons of young and mature rats. Reverse transcriptase-polymerase chain reaction and immunoblotting analyses show that the expression of Ptch and Smo remains at a moderate level in young postnatal and adult brains. By using immunofluorescence light microscopy and immunoelectron microscopy, we examine the spatial distribution of Ptch and Smo within the hippocampal neurons. In young developing neurons, Ptch and Smo are present in the processes and are clustered at their growth cones. In mature neurons, Ptch and Smo are concentrated in dendrites, spines, and postsynaptic sites. Synaptic Ptch and Smo often co-exist with unusual structures—synaptic spinules and autophagosomes. Our results reveal the anatomical organization of the Shh receptors within both the young and the mature hippocampal neurons.

INDEXING TERMS

Sonic hedgehog; Patched; Smoothened; hippocampal neuron; synapse; synaptic spinule; autophagosome; primary cilium

Sonic hedgehog (Shh) signaling plays a pivotal role in the pattern formation of many embryonic tissues (Ingham and McMahon, 2001), and also in homeostasis and regeneration of adult tissues (Beachy et al., 2004). During Shh signaling, Shh proteins bind to a 12-span transmembrane protein, Patched (Ptch), consequently lessening Ptch-mediated suppression of a 7-span transmembrane protein, Smoothened (Smo). Smo, a G protein-coupled receptor-like protein, in turn activates the Gli family of transcription factors (Varjosalo and Taipale, 2008; Zheng et al., 2010).

In the nervous system of young and adult animals, Shh is known to stimulate the proliferation of cerebellar granule cell precursors (Dahmane and Ruiz i Altaba, 1999; Wallace, 1999; Wechsler-Reya and Scott, 1999; Vaillant and Monard, 2009) as well as

*CORRESPONDENCE TO: Pamela J. Yao, Ph. D., Laboratory of Neurosciences, NIA/NIH Biomedical Research Center, 251 Bayview Boulevard, Baltimore, MD 21224. yaopa@grc.nia.nih.gov.

neural progenitors residing in the subventricular zone of the forebrain (Palma et al., 2005; Breunig et al., 2008) and in the dentate gyrus of the hippocampus (Lai et al., 2003; Han et al., 2008). In addition to acting as a mitogen for cells with stem-cell-like properties, Shh also promotes the growth of axons of young neurons soon after they are generated from progenitor cells. This aspect of Shh in axonal growth has been demonstrated in several types of neurons, including spinal cord commissural neurons (Charron et al., 2003; Parra and Zou, 2010), retinal ganglion cells (Trousse et al., 2001), olfactory sensory neurons (Gong et al., 2009; Chou et al., 2010), and midbrain dopaminergic neurons (Hammond et al., 2009). However, whether Shh signaling plays roles in the development of the postmitotic neurons in the hippocampus is not known.

In this study we assessed the expression levels of Shh, Ptch, and Smo in postnatal and adult brains, including the hippocampus. We then focused on Ptch and Smo and examined their distribution in cultured hippocampal neurons. We further examined the spatial distribution of Ptch and Smo in vivo within both the young and mature hippocampal neurons by using immunoelectron microscopy. We found that in young hippocampal neurons, Ptch and Smo are present in the processes and growth cones. In mature hippocampal neurons, Ptch and Smo are located predominately in dendrites, dendritic spines, and postsynaptic sites.

MATERIALS AND METHODS

Animals

All animal procedures were approved by the National Institute on Aging and NIDCD Animal Care and Use Committee and complied with the NIH Guide for Care and Use of Laboratory Animals. Timed pregnant female Sprague-Dawley rats were used as the source of cultured hippocampal cells.

Cultured hippocampal neurons

Cultures of hippocampal neurons were prepared from embryonic day 17 rat brains as described previously (Mattson et al., 1989; Bushlin et al., 2008). Dissociated neurons were plated at a low density (<100 cells/mm^2) on coverslips coated with poly-D-lysine. The neurons were grown in Neurobasal medium/B27 (Invitrogen, Carlsbad,CA). For the transfection experiments, neurons were transfected by using the calcium phosphate-based method and analyzed 2–3 days later.

Antibody characterization

Table 1 lists all antibodies used. The antibody to Ptch was produced against a region of human Ptch that has a high sequence homology between human and rodent. This antibody has been shown to label the commissural axons of embryonic mouse and dissociated dorsal spinal neurons, both of which are Shh-responsive cells (Parra and Zou, 2010). In the present study, we confirmed the specificity of this Ptch antibody by demonstrating that it recognized the expected ~130-kDa band on immunoblots from tissue lysates of rat hippocampus and cerebellum and that the band was absent in the lysates of Ptch−/− MEFs (mouse embryonic fibroblasts; Fig. 1B).

The antibody to Smo was produced against a region of human Smo (Abcam, Boston, MA) that has a high sequence homology among vertebrates. We confirmed the specificity of the antibody by demonstrating the presence of the expected ~80-kDa band in the lysates of Smo-transfected cells and the absence of the same band in Smo−/− MEFs (Fig. 1C).

The antibody to β-actin staining a single band of ~50 kDa on immunoblots has been characterized by Liao et al. (2000), and is widely used for monitoring protein loading in immunoblotting.

The Smi312 antibody selectively recognizes an epitope of nonphosphorylated neurofilaments. The specificity of the antibody has been demonstrated by multiple methods including two-dimensional immunoblots of rat brain tissues following trypsin and phosphatase digestion (Sternberger and Sternberger, 1983). In this study, we show that the antibody labels the axons of the hippocampal neurons—a pattern consistent with previous reports (i.e., Mai et al., 2009).

The microtubule-associated protein 2 (MAP2) antibody recognizes all isoforms of MAP2, as illustrated in sodium dodecyl sulfate-polyacrylamide gel electrophoresis (SDS-PAGE) analysis of bovine brain tissues (Aizawa et al., 1989). In this study, we find that the antibody selectively labels the dendrites of hippocampal neurons, consistent with previous reports of rat neurons (Huber and Matus, 1984; Mai et al., 2009).

The antibody to bassoon detects a band of ~400 kDa on immunoblots, and also selectively labels presynaptic terminals revealed by both light microscopy and electron microscopy (Tom Dieck et al., 1998; Richter et al., 1999). The bassoon immunolabeling pattern found in this study is consistent with the previous reports.

The antibody to adenylyl cyclase III (ACIII) detects a band of ~180–190 kDa on immunoblots of cell lysates from mouse olfactory cilia (Wei at al., 1998). The antibody has also been shown to label the primary cilium, in neurons including olfactory sensory neurons (Rodriguez-Gil and Greer, 2008) and hippocampal neurons (Berbari et al., 2007). Consistently, we find the ACIII antibody specifically labels the primary cilium in neurons of this study.

Cell lines and DNA constructs

Ptch−/− mouse embryonic fibroblasts (MEFs) and wild-type MEFs were kindly provided by Dr. Matthew P. Scott (Stanford University, Palo Alto, CA), and Smo−/− MEFs (4C20) were kindly provided by Dr. Philip A. Beachy (Stanford University). Ptch-YFP and Smo-cMyc were gifts from Dr. James K. Chen (Stanford University), and Smo-EGFP was obtained from Addgene. Ptch-YFP and Smo-AQ1 EGFP contain fluorescent proteins at the C terminus; Smo-cMyc contains three consecutive Myc epitopes at the protein C terminus; all constructs were verified by DNA sequencing (Taipale et al., 2000; Chen et al., 2002; Hyman et al., 2009).

RT-PCR

The RNA extraction and cDNA generation from whole brains (E12 and E14) and the cortex regions (E18 and P2) were the same as described previously (Schwartz et al., 2010). Briefly, immediately following total RNA extraction using Trizol, cDNA was synthesized with Superscript First-Strand Strand Synthesis System (Invitrogen). Reverse transcriptase-polymerase chain reaction (RT-PCR) of Shh, Ptch, and Smo transcript expression was carried out by using the following components: 1 ml of cDNA diluted 1:10 in DEPC water, 1 ml of 10 mM forward primer, 1 ml of 10 mM reverse primer, 22 ml of DEPC water, 25 ml of RedTaq (Sigma-Aldrich, St. Louis, MO). The thermal cycling parameters for the PCR reactions were as follows: an initial denaturation for 3 minutes at 94°C followed by denaturation for 1 minute at 94°C; annealing for 1 minute at 60°C; extension for 1 minute at 72°C, and final extension for 7 minutes at 72°C; 30 or 35 cycles were used for reactions. The PCR primers were all designed against rat by using NCBI Primer Blast and obtained from IDT DNA. The sequences are: Shh, 5′-AAGGAGGAGCGCACACGCAC-3′ and 5′-

TTGGCACCTTCGTC GCGGTC-3′; Ptch, 5′-CTGCGTCACTGGCTGCTGCT-3′ and 5′-GCCGGTTTAGGCCGTTGGCT-3′; Smo, 5′-GCAGGAGGAAGCGCACAGCA-3′ and 5′-GGAAGTGGTCCGGCGTGCAA-3′. To ensure that RNAs were not contaminated with genomic DNA, cDNAs were tested by running the reverse transcriptase reaction without SuperScript III and PCR was carried out with GAPDH primers as recommended by the manufacturer.

Immunoblots

Tissue lysates were prepared as described (Petralia and Yao, 2007). Briefly, tissues were lysed in an ice-cold buffer containing a protease inhibitor cocktail tablet (Roche Applied Science, Indianapolis, IN). An equal amount of total protein from each sample was subjected to SDS-PAGE and immunoblotting analysis by using standard procedures. The Ptch and Smo antibodies were used at 1:200, and β-actin antibody was used at 1:5,000 (Table 1).

Immunocytochemistry and fluorescence microscopy

Immunofluorescence labeling was carried out as described previously (Bushlin et al., 2008). Neurons were fixed with 4% paraformaldehyde and 4% sucrose for 15 minutes, washed, and then permeabilized with 0.1% Triton X-100. After blocking, the neurons were incubated overnight with a primary antibody at 4°C. The dilutions of the antibodies used are listed in Table 1. The neurons were then washed and incubated with an appropriate fluorescently tagged secondary antibody. The labeled neurons were examined by using a 40× or a 63× objective on a Zeiss LSM510 laser scanning confocal microscope. All images were acquired at a 1,024 × 1,024 pixel resolution. The brightness, contrast, and levels of the images were minimally adjusted (in Adobe Photoshop 8.0) for those images presented. No additional digital image processing was performed.

Immunoelectron microscopy

Preembedding EM immunoperoxidase/diaminobenzidine (DAB) labeling was performed following established methods (Petralia and Wenthold, 1999; Petralia et al., 2010). Briefly, after blocking in 10% normal goat serum, tissue sections were incubated with primary antibody overnight at 4°C and then processed for immunoperoxidase labeling by using a Vectastain kit and ImpacDAB (Vector, Burlingame, Ca). The following dilutions were used for the primary antibodies: Ptch rabbit serum, 1:2,000; Smo rabbit serum, 1:500 to 1:1,000. Sections were washed in cacodylate buffer, fixed in 2% glutaraldehyde, then in 1% osmium tetroxide, dehydrated in alcohols and propylene oxide, and embedded in Epon. Thin sections were cut on a Leica Ultracut ultramicrotome (Vienna, Austria) and examined with a JEOL JSM-1010 EM (Peabody, MA) and AMT digital camera (Danvers, MA).

Postembedding immunogold labeling was performed by using established methods (Petralia and Wenthold, 1999; Bushlin et al., 2008; Petralia et al., 2010). Following cryoprotection and embedding, tissue sections were further processed and embedded in Lowicryl HM-20 resin by using a Leica AFS freeze-substitution instrument. After blocking, sections were incubated with the primary antibody. The following concentrations were used for the primary antibodies: Ptch rabbit serum, 1:100; Smo rabbit serum, 1:100 to 1:500. Following incubation with 10 nm gold-conjugated secondary antibody, the sections were stained with uranyl acetate and lead citrate.

All regions studied with either immunoperoxidase/DAB or immunogold were examined in two to three animals per method. The following lists the number of images examined by antibody/region: Ptch/immunogold P2 hippocampus, 86; Smo/immunogold P2 hippocampus, 131; Ptch/DAB adult hippocampus, 202; Smo/DAB adult hippocampus, 213;

Ptch/immunogold adult hippocampus, 213; Smo/immunogold, 129; Ptch/immunogold choroid plexus, 22; Smo/immunogold P2 choroid plexus, 25; thus the total is 1,021. For all electron microscopy methods, images were stored in their original formats and final images for figures were prepared in Adobe Photoshop; levels and brightness/contrast of images were minimally and evenly adjusted over the entire micrograph. Control sections for immunogold or immunoperoxidase methods omitting the primary antibody showed only rare gold labeling or DAB reaction product.

RESULTS

Ptch and Smo are expressed in the developing and mature hippocampus

We began our study by examining the expression of Shh and its receptors, Ptch and Smo, in embryonic and postnatal brains. RT-PCR analysis showed that Shh, Ptch, and Smo mRNAs are expressed at high levels in rat brains between embryonic day (E) 12 and postnatal day (P) 2 (Fig. 1A), a temporal expression pattern consistent with in situ hybridization analysis (Allen Brain Atlas; http://www.brain-map.org). Spatially, the in situ hybridization analysis (Allen Brain Atlas) also reveals the expression of Ptch and Smo mRNA in postmitotic neurons of the hippocampus, where the functional significance of Shh signaling is not well understood.

We focused on Ptch and Smo for further studies. We assessed the protein levels of Ptch and Smo in the hippocampus and cerebellum from P2 and adult (P35) rats by using immunoblotting analysis. We used a Ptch antibody that has been demonstrated to label Ptch protein in spinal cord commissural neurons (Parra and Zou, 2010). Assay of the brain lysates using this antibody revealed a protein band of ~130 kDa, the expected size for rat Ptch1 (Fig. 1B). The ~130-kDa protein band was present in wild-type MEFs but absent in Ptch−/− MEFs (Fig. 1B), confirming the specificity of the antibody. We found that Ptch proteins were detectable in both P2 and adult rat brains, although the expression levels were higher in the hippocampus than in the cerebellum (Fig. 1B).

The same brain lysates were analyzed for Smo protein levels. The Smo antibody recognized a protein band of ~80 kDa (Fig. 1C), the expected size for rat Smo. The specificity of the Smo antibody was verified by the detection of the same Smo protein band in lysates of HEK293 cells expressing a Smo cDNA construct and of wild-type MEFs, and by the lack of the band in Smo−/− MEFs (Fig. 1C). The levels of Smo were similar in the hippocampus and the cerebellum at both P2 and P35 (Fig. 1C).

Ptch and Smo are present in young and mature hippocampal neurons

Having verified the expression of Ptch and Smo proteins in the postnatal brain, we proceeded to focus the present study on the hippocampal neurons. To assess the expression pattern of Ptch and Smo in postmitotic neurons, we immunolabeled Ptch and Smo in cultured hippocampal neurons, a model system that has been widely used to study signaling pathways in neuronal growth. We first examined young hippocampal neurons grown in culture for ~2 days (2 div). By this culture stage, a typical neuron will have developed a single axon and multiple dendrites (Mattson et al., 1989). We immunolabeled Ptch or Smo in these neurons along with the axonal marker Smi312 or the dendritic marker MAP2. In addition to being seen in the soma, faint but positive Ptch immunolabeling was visible in the tips of MAP2-labeled dendrites (denoted by white arrowheads in Fig. 2A,B), presumably dendritic growth cones. Likewise, the Smo immunolabeling was bright and intense in the distal sections of dendrites (white arrowheads in Fig. 2C,D). There was some Smo labeling at tips of the Smi312-expressing axon (denoted by yellow arrowhead in Fig. 2C), although the axonal labeling appeared weaker than the dendritic labeling.

We next examined hippocampal neurons grown in culture for at least 20 days. Typical mature neurons at this culture stage have well-developed dendrites and spines. We found positive Ptch immunolabeling in dendrites and spines (Fig. 2E,F). The bright Ptch labeling in spines was closely apposed to presynaptic puncta labeled with a presynaptic marker, bassoon (white arrowheads in Fig. 2F). Smo immunolabeling, on the other hand, was mostly seen in dendrites (Fig. 2G,H).

We also examined hippocampal neurons expressing Smo-cMyc. In young neurons, the ectopically expressed Smo-cMyc was found in the soma, but also in dendritic (white arrowheads) and axonal (yellow arrowhead) growth cones (Fig. 2I,J). In mature neurons, ectopic Smo was far higher in dendrites than in spines (Fig. 2K,L). Thus, the expression pattern of ectopic Smo is similar to that of endogenous Smo.

Ultrastructural localization of Ptch and Smo in young hippocampal neurons

To further identify the subcellular distribution of Ptch and Smo in the young hippocampal neurons in vivo, we performed immunogold electron microscopy on the hippocampus (focusing on CA1) of P2 rats. Both Ptch and Smo immunogold particles were readily found in young neurons, particularly in the growth cones of the neurons (Fig. 3). Growth cones were defined as large balloon-shaped processes that contain noticeable ovoid-shaped organelles (endosomes) and that lack the organized central microtubule array of axon and dendrite shafts. A striking feature of the Ptch- and Smo-containing neurons was the presence of copious intermediate filaments (~10 nm) and microtubules (~25 nm) (Fig. 3)—a well-characterized trait of migrating, newly generated neurons (Butler and Caley, 1972; Kaplan and Bell, 1984; Zerlin et al., 1995). Within these young neurons, we found that Ptch immunogold particles located at the plasma membrane where it formed membrane appositions between growth cones or shafts of immature neuronal processes (Fig. 3A,B,D,I). Some of the Ptch-containing growth cones or processes were dendritic (large and tapering shaft with central microtubules and organelles; Fig. 3A,B) or axonal (thin and nontapering shaft; Fig. 3I), whereas others did not display the typical features of either dendrites or axons (Fig. 3D).

Like Ptch, Smo was also present in the processes (Fig. 3C,H), growth cones (Fig. 3E,J), and even nascent synaptic terminals (i.e., those bearing few presynaptic vesicles and exhibiting a thin postsynaptic density; Fig. 3F), of newly generated neurons. In addition to the plasma membrane, Smo was often associated with a variety of cytoplasmic organelles, including clathrin-coated vesicles (Fig. 3C) and different types of endosomes (Fig. 3E,H,J). The clathrin-coated vesicles were identified by the characteristic ring of " T-shaped" coating structures, and endosomes were seen as profiles of large ovoid organelles, often showing a tubular extension on one of both ends.

Ultrastructural localization of Ptch and Smo in mature hippocampal neurons

To examine the subcellular distribution of Ptch and Smo in the mature hippocampus, we performed preembedding immunoperoxidase/DAB and postembedding immunogold labeling in adult rats (P35–37). First, we surveyed immunoperoxidase/DAB-labeled tissues by using light microscopy. For Ptch labeling, we observed densely packed and darkly labeled Ptch puncta, many of which were associated with, or extended from, lightly labeled dendrites (Fig. 4A,C,E,G). This labeling pattern was similar in all three regions of the hippocampus examined, including the CA1 (Fig. 4A,C), the dentate gyrus (Fig. 4E), and the CA3 (Fig. 4G). For Smo labeling, however, we observed a pattern distinctly different from Ptch: intensely labeled dendrites but lightly, and only occasionally moderately, labeled puncta (Fig. 4B,D,F,H) across all three hippocampal regions. Notably, for both Ptch and Smo labelings, we did not see definitively labeled axons. Furthermore, of the three

hippocampal regions examined, we did not find unambiguous Ptch or Smo labeling in glial cells.

The above light microscopic analyses of in vitro cultured hippocampal neurons (Fig. 2C,D,F) and in vivo hippocampal tissues (Fig. 4) suggested that Ptch and Smo are present at the synapses of mature neurons. Therefore, we next focused on further examining the synaptic distribution of Ptch and Smo by using electron microscopy. We found that, in classic spine synapses such as those found in the CA1 and CA3 stratum radiatum of the adult hippocampus, Ptch-immunoreactive DAB products were predominately situated in spine heads (Fig. 5A,B). (Spine head profiles were defined by the presence of a postsynaptic density opposed to a presynaptic terminal containing synaptic vesicles and an active zone; spine heads lack definitive features of dendrite shafts such as microtubules and mitochondria.) In contrast, the nearby dendrites—including the dendrites from which the Ptch-positive spines were derived—had little Ptch immunolabeling (Fig. 5A,B). Smo immunolabeling, in contrast, was seen in dendrites in addition to spines. In some synapses, Smo labeling was more intense in dendrites than in spines (Fig. 5C,H), whereas in other synapses, spine Smo was noticeable (Fig. 5D and inset). We also examined postembedding immunogold-labeled tissues. Consistent with the DAB labeling, Ptch immunogold particles were frequently found in spines (Fig. 5E,F), whereas Smo immunogold particles were present in some spines but were far more abundant in dendrites (Fig. 5G,I).

We next examined spine synapses in the dentate gyrus area of the hippocampus. The Ptch and Smo distribution patterns in dentate spine synapses (Fig. 6) were identical to those in the CA1 and CA3 spine synapses (Fig. 5) described above: Ptch was enriched in spines (Fig. 6A,C, E–G), whereas Smo was found in dendrites (Fig. 6D,H) and in spines (Fig. 6B,D).

We wondered whether the postsynaptic locations of Ptch and Smo were unique to classic spine synapses or could also be found in other types of synapses. To address this question, we examined the CA3 mossy fiber synapse where large convoluted mossy terminals, containing large numbers of synaptic vesicles and multiple active zones, synapse with complex postsynaptic thorny excrescences. Thorny excrescences are large irregular extensions from the dendrite shaft, making multiple synaptic contacts with mossy fiber terminals. Figure 7A shows Ptch-immunoreactive DAB products to be strongly present in postsynaptic thorny excrescences, and concentrated at the synaptic junction. Figure 7D reveals Ptch immunogold particles in thorny excrescences. Figure 7B and C shows the presence of Smo-immunoreactive DAB products in the thorny excrescences as well as in the dendrites, but not in the mossy terminals. Figure 7E reveals Smo immunogold particles in thorny excrescences.

Postsynaptic Ptch and Smo coexist with synaptic spinules and autophagosomes

We also noticed that the mossy synapses housing Ptch or Smo exhibited two additional features. First, they contained synaptic spinules (denoted by an asterisk in Figs. 7A, 8). Synaptic spinules are small membrane protrusions from the postsynaptic terminal into the presynaptic terminal (Westrum and Blackstad, 1962; Tarrant and Routtenberg, 1977) or from axons to neighboring processes (Spacek and Harris, 2004). These spinules are transitory structures and their occurrence is directly correlated to synaptic activity (Tao-Cheng et al., 2009). Therefore, synaptic spinules likely signify highly active synapses (Wagner and Djamgoz, 1993; Tao-Cheng et al., 2009). We observed two types of spinules: small finger-like and large spine-like spinules, both of which had two clearly traceable layers of plasma membranes and protruded in the midst of synaptic vesicles within the mossy terminals (Figs. 7A, 8A,C,F). In the small finger-like spinules, Ptch did not reside inside spinules but was stationed in the nearby structures (Figs. 7A, 8A), whereas in the

large spine-like spinules, Ptch (Fig. 8C), as well as Smo (Fig. 8F), was found within these spinule structures.

A second notable feature of the mossy synapses containing Ptch and Smo was the presence of autophago-some-like structures (denoted by double asterisks in Figs. 7B, 8). Autophagosomes are bulk degenerative processes consisting of multilayered, sometimes irregularly folded, membranes. Autophagosomes and the process of autophagy have diverse physiological functions including synaptic development and plasticity (Shen and Ganetzky, 2009). In the mossy terminals, we found large multilayered lamellar degenerative structures resembling autophagosomes (Hayashi-Nishino et al., 2009). We also observed that these autophagosome-like structures contained Ptch and Smo (Figs. 7B, 8). Furthermore, as clearly revealed in Figure 8B,D,E, Ptch is located on the membranes of autophagosomes.

We draw three conclusions from these results. First, in young hippocampal neurons, Ptch and Smo are expressed in growth cones of axons and dendrites. Second, in mature hippocampal neurons, Ptch and Smo become enriched in the dendrites and spines. Third, Ptch and Smo coexist and closely associate with dynamic synaptic structures such as spinules and autophagosomes.

Ptch and Smo are present in the primary cilium of the neuron

It has been established that the localization of Ptch and Smo to the primary cilium is essential to Shh signaling in mammalian cells (Corbit et al., 2005; Kim et al., 2009; Wang et al., 2009; Rohatgi et al., 2010). We analyzed the expression of Ptch and Smo in relation to the primary cilium in neurons. Our goal was not to comprehensively investigate the neuronal cilium—an area that is currently less understood—but to ascertain whether the primary cilium in postmitotic neurons contained Ptch and Smo. We focused on young neurons that had grown in culture for 2–4 days. Because acetylated α-tubulin—the conventional marker for non-neuronal cilia—is nonspecific for neurons (Berbari et al., 2007; and data not shown), we labeled neurons with an antibody to adenylyl cyclase III (ACIII), a marker shown to be useful for visualizing primary cilia in neurons (Berbari et al., 2007; Bishop et al., 2007). We found that only a subset of neurons (33% ± 5, n = 400 cells) possessed ACIII-labeled cilia (Fig. 9A–F). We also examined the neurons expressing Smo-epidermal growth factor protein (EGFP). Comparing ACIII-labeled neurons with Smo-EGFP-expressing neurons, we found that ACIII labeled some but not all Smo-GFP-containing cilia (Fig. 9A–F).

Because of the incompatibility of the available antibodies, we were unable to perform double immunolabeling of ACIII with Ptch or Smo. However, we immunolabeled Ptch and Smo in neurons containing Smo-EGFP-expressing cilia. Both Ptch (Fig. 9G–L) and Smo (Fig. 9M–R) immunolabelings were detected in, although not exclusively confined to, the cilia. In addition, the distribution of Smo immunolabeling correlated with the distribution of Smo-EGFP, again confirming the specificity of the Smo antibody.

We next performed Smo immunogold labeling in the choroid plexus located rostral to the hippocampus of P2 rats. We chose the choroid plexus for two reasons. First, at the ultrastructural level, identifying a primary cilium is considerably more feasible in the choroid plexus region than within the hippocampal parenchyma. Second, Shh signaling has been shown to take place in the choroid plexus (Traiffort et al., 1999; Huang et al., 2009; Nielsen and Dymecki, 2010). Figure 9S shows the cross-section view of a cilium and Figure 9T a longitudinal view of a cilium, both of which were in the midst of microvilli and—more importantly—both of which contained Smo immunolabelings. Note that Smo labeling was also found associated with trafficking organelles such as clathrin-coated vesicles located at the base of the microvilli (Fig. 9U). Thus, although our understanding of the primary cilium

in neurons is far from complete, our finding suggests that neuronal cilia could play a role in Shh signaling similar to that of non-neuronal cilia.

DISCUSSION

We have examined the expression level and subcellular localization of Shh's dual receptors, Ptch and Smo, in the young and mature hippocampal neurons. Ptch and Smo continue to be present in the postnatal and adult hippocampus, implying a novel role for continuous Shh signaling in the hippocampus beyond the stage of embryonic development. Light and electron microscopy analyses provide a coarse overview and a detailed characterization of Ptch and Smo localization in the hippocampal neurons.

Although previous studies have described the expression of Ptch in the hippocampus (Traiffort et al., 1999; Lai et al., 2003), this study is the first that examines and reveals the distribution of Ptch protein at the subcellular level within the hippocampal neurons. One previous study reported Smo's "exclusively" presynaptic expression in the hippocampal mossy terminal (Masdeu et al., 2007; reviewed in Traiffort et al., 2010). However, we find that Ptch and Smo are present predominately in the spines and dendrites of hippocampal neurons; this pattern is seen in vitro of cultured neurons and in vivo of different types of synapses in several regions of the hippocampus (Figs. 2–8).

There are several lines of evidence that support our findings. First, we characterized and demonstrated the specificity of the Ptch and Smo antibodies (Fig. 1B,C). Second, in situ hybridization analysis from the Allen Brain Atlas (http://www.brain-map.org) and a recent report (Sasaki et al., 2010) show clearly detectable transcripts for Ptch as well as for Smo in the CA1 and CA3 pyramidal neurons, consistent with our findings of Ptch and Smo proteins in these neurons. Third, Sasaki et al. (2010) also showed an interaction between Smo and Tiam1—a known postsynaptic protein that regulates spine formation in hippocampal neurons (Tolias et al., 2005, 2007)—supporting our observations of Smo in the spines and dendrites. Fourth, we examined several hippocampal areas, including the CA1 stratum radiatum and stratum oriens, the CA3 stratum radiatum, the CA3 stratum lucidum (mossy terminal area), and the molecular layer of the dentate gyrus. In the synapses of all these areas, we observed the same pattern: Ptch and Smo were present on the postsynaptic side of the synapses. Fifth, in cultured hippocampal neurons, we detected endogenous Ptch and Smo, as well as ectopically expressed Smo-cMyc, in the spines and dendrites. Lastly, the detection of Ptch and Smo in the primary cilium of hippocampal neurons in vitro (Fig. 9A–H) and of choroid plexus in vivo (Fig. 9I)—the structures where Shh signaling is known to take place and the expression of Ptch and Smo has been shown (Traiffort et al., 1999; Huang et al., 2009; Nielsen and Dymecki, 2010)—further supports the specificity of our Ptch and Smo labeling.

Shh signaling has been shown to control neural stem cells in postnatal and adult brains (Lai et al., 2003; Palma et al., 2005; Breunig et al., 2008; Han et al., 2008). The present study did not focus on those neural stem cells that reside in the subgranular layers of the hippocampal dentate gyrus, but rather, focused on the hippocampal cells that have differentiated into neurons. The presence of Ptch and Smo in newly generated migrating neurons and the location of Ptch and Smo in the growth cones of these neurons (Figs. 2, 3) suggest that Shh signaling could contribute to or control the growth of these neurons, much like Shh's role in axonal growth of other types of neurons (Trousse et al., 2001; Charron et al., 2003; Gong et al., 2009; Hammond et al., 2009; Chou et al., 2010; Parra and Zou, 2010). However, whether Shh signaling regulates axonal or dendritic growth, where and how Shh is produced, and the underlying mechanisms involved, will all require further study.

Our finding that Ptch and Smo localize at the synapses provides new insights into the function of Shh signaling in the mature hippocampal neurons. The coexistence of Ptch and Smo in the dendrites and spines of several hippocampal areas is worth emphasizing because it raises the possibility not only that Shh signaling takes place at the synapses, but also that the postsynaptic compartments harbor the receptors for the signaling, at least in the hippocampal neurons. It is possible that Shh, similar to Wnt—another embryonic morphogen—has roles in synaptic development and function (Speese and Budnik, 2007).

Another feature of the Ptch- and Smo-containing synapses is the presence of two unusual synaptic structures: synaptic spinules and autophagosomes (Figs. 7, 8). Although the ultrastructure of synaptic spinules has been meticulously described (Westrum and Blackstad, 1962; Tarrant and Routtenber, 1977; Spacek and Harris, 2004), the functions of these structures remain mostly unknown. It has been suggested that synaptic spinules could represent a form of trans-endocytosis (Spacek and Harris, 2004; Yao et al., 2005) that transmit retrograde signaling from dendrites to the cell body and axons. Because of their transient and dynamic nature, it has also been suggested that synaptic spinules could play an active role in remodeling the synapses (Wagner and Djamgoz, 1993; Tao-Cheng et al., 2009). The finding of Ptch and Smo in spinule-containing adult synapses suggests that Shh signaling may be involved in synaptic remodeling and plasticity.

Autophagy, a lysosome-dependent degradation mechanism, has major roles in protein and organelle turnover that are likely a crucial part of tissue homeostasis and regeneration. Although it has been suggested that, in the nervous system, autophagy is involved in synapse development (Shen and Ganetzky, 2009) and neuron degeneration (Martinez-Vicente and Cuervo, 2007), the roles of autophagosomes in the mammalian neurons and their synapses are unknown. Our ultrastructural analysis reveals an intimate anatomical relationship between the receptors for Shh and autophagosomes in the synapses of hippocampal neurons (Figs. 7, 8). Extrapolating from this observation, it seems possible that Shh signaling influences the process of autophagy in synaptic compartments, yet a reverse relationship—in which autophagy would control Shh signaling—is also equally possible. A recent study has demonstrated that autophagy regulates Wnt signaling by degrading Wnt's receptor, Dishevelled, resulting in Wnt inhibition (Gao et al., 2010). Although it is tempting to speculate that a similar regulatory mechanism is utilized by the Shh signaling pathway, a definitive answer will require further investigation.

Acknowledgments

We are grateful to Dr. Roger H. Reeves whose interest in Sonic hedgehog and neural development inspired us. We thank Drs. James K. Chen, Matthew P. Scott, and Philip A. Beachy for generously providing reagents. We also thank Dr. Carolyn Marie Ott for valuable discussions on the primary cilium and Dr. Fred E. Indig for confocal microscopy.

Grant sponsor: Intramural Research Programs of the National Institute on Aging and the National Institute on Deafness and Other Communication Disorders, National Institutes of Health.

LITERATURE CITED

Aizawa H, Kawasaki H, Murofushi H, Kotani S, Suzuki K, Sakai H. A common amino acid sequence in 190-kDa microtubule-associated protein and tau for the promotion of microtubule assembly. J Biol Chem. 1989; 264:5885–5890. [PubMed: 2494169]

Beachy PA, Karhadkar SS, Berman DM. Tissue repair and stem cell renewal in carcinogenesis. Nature. 2004; 432:324–331. [PubMed: 15549094]

Berbari NF, Bishop GA, Askwith CC, Lewis JS, Mykytyn K. Hippocampal neurons possess primary cilia in culture. J Neurosci Res. 2007; 85:1095–1100. [PubMed: 17304575]

Bishop GA, Berbari NF, Lewis J, Mykytyn K. Type III adenylyl cyclase localizes to primary cilia throughout the adult mouse brain. J Comp Neurol. 2007; 505:562–571. [PubMed: 17924533]

Breunig JJ, Sarkisian MR, Arellano JI, Morozov YM, Ayoub AE, Sojitra S, Wang B, Flavell RA, Rakic P, Town T. Primary cilia regulate hippocampal neurogenesis by mediating sonic hedgehog signaling. Proc Natl Acad Sci U S A. 2008; 105:13127–13132. [PubMed: 18728187]

Bushlin I, Petralia RS, Wu F, Harel A, Mughal MR, Mattson MP, Yao PJ. Clathrin assembly protein AP180 and CALM differentially control axogenesis and dendrite outgrowth in embryonic hippocampal neurons. J Neurosci. 2008; 28:10257–10271. [PubMed: 18842885]

Butler AB, Caley DW. An ultrastructural and radioautographic study of the migrating neuroblast in hamster neocortex. Brain Res. 1972; 44:83–97. [PubMed: 5056990]

Charron F, Stein E, Jeong J, McMahon AP, Tessier-Lavigne M. The morphogen sonic hedgehog is an axonal chemoattractant that collaborates with netrin-1 in midline axon guidance. Cell. 2003; 113:11–23. [PubMed: 12679031]

Chen JK, Taipale J, Cooper MK, Beachy PA. Inhibition of Hedgehog signaling by direct binding of cyclopamine to Smoothened. Genes Dev. 2002; 16:2743–2748. [PubMed: 12414725]

Chou YH, Zheng X, Beachy PA, Luo L. Patterning axon targeting of olfactory receptor neurons by coupled hedgehog signaling at two distinct steps. Cell. 2010; 142:954–966. [PubMed: 20850015]

Corbit KC, Aanstad P, Singla V, Norman AR, Stainier DY, Reiter JF. Vertebrate Smoothened functions at the primary cilium. Nature. 2005; 437:1018–1021. [PubMed: 16136078]

Dahmane N, Ruiz i Altaba A. Sonic hedgehog regulates the growth and patterning of the cerebellum. Development. 1999; 126:3089–3100. [PubMed: 10375501]

Gao C, Cao W, Bao L, Zuo W, Xie G, Cai T, Fu W, Zhang J, Wu W, Zhang X, Chen YG. Autophagy negatively regulates Wnt signalling by promoting Dishevelled degradation. Nat Cell Biol. 2010; 12:781–790. [PubMed: 20639871]

Gong Q, Chen H, Farbman AI. Olfactory sensory axon growth and branching is influenced by sonic hedgehog. Dev Dyn. 2009; 238:1768–1776. [PubMed: 19517566]

Hammond R, Blaess S, Abeliovich A. Sonic hedgehog is a chemoattractant for midbrain dopaminergic axons. PLoS One. 2009; 4:e7007. [PubMed: 19774071]

Han YG, Spassky N, Romaguera-Ros M, Garcia-Verdugo JM, Aguilar A, Schneider- Maunoury S, Alvarez-Buylla A. Hedgehog signaling and primary cilia are required for the formation of adult neural stem cells. Nat Neurosci. 2008; 11:277–284. [PubMed: 18297065]

Hayashi-Nishino M, Fujita N, Noda T, Yamaguchi A, Yoshimori T, Yamamoto A. A subdomain of the endoplasmic reticulum forms a cradle for autophagosome formation. Nat Cell Biol. 2009; 11:1433–1437. [PubMed: 19898463]

Huber G, Matus A. Immunocytochemical localization of microtubule-associated protein 1 in rat cerebellum using monoclonal antibodies. J Cell Biol. 1984; 98:777–781. [PubMed: 6363428]

Huang X, Ketova T, Fleming JT, Wang H, Dey SK, Litingtung Y, Chiang C. Sonic hedgehog signaling regulates a novel epithelial progenitor domain of the hindbrain choroid plexus. Development. 2009; 136:2535–2543. [PubMed: 19570847]

Hyman JM, Firestone AJ, Heine VM, Zhao Y, Ocasio CA, Han K, Sun M, Rack PG, Sinha S, Wu JJ, Solow-Cordero DE, Jiang J, Rowitch DH, Chen JK. Small-molecule inhibitors reveal multiple strategies for Hedgehog pathway blockade. Proc Natl Acad Sci U S A. 2009; 106:14132–14137. [PubMed: 19666565]

Ingham PW, McMahon AP. Hedgehog signaling in animal development: paradigms and principles. Genes Dev. 2001; 15:3059–3087. [PubMed: 11731473]

Kaplan MS, Bell DH. Mitotic neuroblasts in the 9-dayold and 11-month-old rodent hippocampus. J Neurosci. 1984; 4:1429–1441. [PubMed: 6726341]

Kim J, Kato M, Beachy PA. Gli2 trafficking links Hedgehog-dependent activation of Smoothened in the primary cilium to transcriptional activation in the nucleus. Proc Natl Acad Sci U S A. 2009; 106:21666–21671. [PubMed: 19996169]

Lai K, Kaspar BK, Gage FH, Schaffer DV. Sonic hedgehog regulates adult neural progenitor proliferation in vitro and in vivo. Nat Neurosci. 2003; 6:21–27. [PubMed: 12469128]

Liao J, Xu X, Wargovich MJ. Direct reprobing with anti-actin antibody as an internal control for Western blot analysis. Biotechniques. 2000; 28:216–218. [PubMed: 10683726]

Mai J, Fok L, Gao H, Zhang X, Poo MM. Axon initiation and growth cone turning on bound protein gradients. J Neurosci. 2009; 29:7450–7458. [PubMed: 19515913]

Martinez-Vicente M, Cuervo AM. Autophagy and neurodegeneration: when the cleaning crew goes on strike. Lancet Neurol. 2007; 6:352–361. [PubMed: 17362839]

Masdeu C, Bernard V, Faure H, Traiffort E, Ruat M. Distribution of Smoothened at hippocampal mossy fiber synapses. Neuroreport. 2007; 18:395–399. [PubMed: 17435610]

Mattson MP, Guthrie PB, Hayes BC, Kater SB. Roles for mitotic history in the generation and degeneration of hippocampal neuroarchitecture. J Neurosci. 1989; 9:1223–1232. [PubMed: 2564886]

Nielsen CM, Dymecki SM. Sonic hedgehog is required for vascular outgrowth in the hindbrain choroid plexus. Dev Biol. 2010; 340:430–437. [PubMed: 20123094]

Palma V, Lim DA, Dahmane N, Sánchez P, Brionne TC, Herzberg CD, Gitton Y, Carleton A, Alvarez-Buylla A, Ruiz i Altaba A. Sonic hedgehog controls stem cell behavior in the postnatal and adult brain. Development. 2005; 132:335–344. [PubMed: 15604099]

Parra LM, Zou Y. Sonic hedgehog induces response of commissural axons to Semaphorin repulsion during midline crossing. Nat Neurosci. 2010; 13:29–35. [PubMed: 19946319]

Petralia RS, Wenthold RJ. Immunocytochemistry of NMDA receptors. Methods Mol Biol. 1999; 128:73–92. [PubMed: 10320974]

Petralia RS, Yao PJ. AP180 and CALM in the developing hippocampus: expression at the nascent synapse and localization to trafficking organelles. J Comp Neurol. 2007; 504:314–327. [PubMed: 17640037]

Petralia RS, Wang YX, Hua F, Yi Z, Zhou A, Ge L, Stephenson FA, Wenthold RJ. Organization of NMDA receptors at extrasynaptic locations. Neuroscience. 2010; 167:68–87. [PubMed: 20096331]

Richter K, Langnaese K, Kreutz MR, Olias G, Zhai R, Scheich H, Garner CC, Gundelfinger ED. Presynaptic cytomatrix protein bassoon is localized at both excitatory and inhibitory synapses of rat brain. J Comp Neurol. 1999; 408:437–448. [PubMed: 10340516]

Rodriguez-Gil DJ, Greer CA. Wnt/Frizzled family members mediate olfactory sensory neuron axon extension. 2008

Rohatgi R, Milenkovic L, Scott MP. Patched1 regulates hedgehog signaling at the primary cilium. Science. 2010; 317:372–376. [PubMed: 17641202]

Sasaki N, Kurisu J, Kengaku M. Sonic hedgehog signaling regulates actin cytoskeleton via Tiam1-Rac1 cascade during spine formation. Mol Cell Neurosci. 2010; 45:335–344. [PubMed: 20654717]

Schwartz CM, Cheng A, Mughal MR, Mattson MP, Yao PJ. Clathrin assembly proteins AP180 and CALM in the embryonic rat brain. J Comp Neurol. 2010; 518:3803–3818. [PubMed: 20653035]

Shen W, Ganetzky B. Autophagy promotes synapse development in *Drosophila*. J Cell Biol. 2009; 187:71–79. [PubMed: 19786572]

Spacek J, Harris KM. Trans-endocytosis via spinules in adult rat hippocampus. J Neurosci. 2004; 24:4233–4241. [PubMed: 15115819]

Speese SD, Budnik V. Wnts: up-and-coming at the synapse. Trends Neurosci. 2007; 30:268–275. [PubMed: 17467065]

Sternberger LA, Sternberger NH. Monoclonal antibodies distinguish phosphorylated and nonphosphorylated forms of neurofilaments in situ. Proc Natl Acad Sci U S A. 1983; 80:6126–6130. [PubMed: 6577472]

Taipale J, Chen JK, Cooper MK, Wang B, Mann RK, Milenkovic L, Scott MP, Beachy PA. Effects of oncogenic mutations in Smoothened and Patched can be reversed by cyclopamine. Nature. 2000; 406:1005–1009. [PubMed: 10984056]

Tao-Cheng JH, Dosemeci A, Gallant PE, Miller S, Galbraith JA, Winters CA, Azzam R, Reese TS. Rapid turnover of spinules at synaptic terminals. Neuroscience. 2009; 160:42–50. [PubMed: 19248820]

Tarrant SB, Routtenberg A. The synaptic spinule in the dendritic spine: electron microscopic study of the hippocampal dentate gyrus. Tissue Cell. 1977; 9:461–473. [PubMed: 337572]

Tolias KF, Bikoff JB, Burette A, Paradis S, Harrar D, Tavazoie S, Weinberg RJ, Greenberg ME. The Rac1-GEF Tiam1 couples the NMDA receptor to the activity-dependent development of dendritic arbors and spines. Neuron. 2005; 45:525–538. [PubMed: 15721239]

Tolias KF, Bikoff JB, Kane CG, Tolias CS, Hu L, Greenberg ME. The Rac1 guanine nucleotide exchange factor Tiam1 mediates EphB receptor-dependent dendritic spine development. Proc Natl Acad Sci U S A. 2007; 104:7265–7270. [PubMed: 17440041]

Tom Dieck S, Sanmartí-Vila L, Langnaese K, Richter K, Kindler S, Soyke A, Wex H, Smalla KH, Kämpf U, Fränzer JT, Stumm M, Garner CC, Gundelfinger ED. Bassoon, a novel zinc-finger CAG/glutamine-repeat protein selectively localized at the active zone of presynaptic nerve terminals. J Cell Biol. 1998; 142:499–509. [PubMed: 9679147]

Traiffort E, Charytoniuk D, Watroba L, Faure H, Sales N, Ruat M. Discrete localizations of hedgehog signalling components in the developing and adult rat nervous system. Eur J Neurosci. 1999; 11:3199–3214. [PubMed: 10510184]

Traiffort E, Angot E, Ruat M. Sonic Hedgehog signaling in the mammalian brain. J Neurochem. 2010; 113:576–590. [PubMed: 20218977]

Trousse F, Martí E, Gruss P, Torres M, Bovolenta P. Control of retinal ganglion cell axon growth: a new role for Sonic hedgehog. Development. 2001; 128:3927–3936. [PubMed: 11641217]

Vaillant C, Monard D. SHH pathway and cerebellar development. Cerebellum. 2009; 8:291–301. [PubMed: 19224309]

Varjosalo M, Taipale J. Hedgehog: functions and mechanisms. Genes Dev. 2008; 22:2454–2472. [PubMed: 18794343]

Wagner HJ, Djamgoz MB. Spinules: a case for retinal synaptic plasticity. Trends Neurosci. 1993; 16:201–206. [PubMed: 7688159]

Wallace VA. Purkinje-cell-derived Sonic hedgehog regulates granule neuron precursor cell proliferation in the developing mouse cerebellum. Curr Biol. 1999; 9 445-228.

Wang Y, Zhou Z, Walsh CT, McMahon AP. Selective translocation of intracellular Smoothened to the primary cilium in response to Hedgehog pathway modulation. Proc Natl Acad Sci U S A. 2009; 106:2623–2628. [PubMed: 19196978]

Wechsler-Reya RJ, Scott MP. Control of neuronal precursor proliferation in the cerebellum by Sonic Hedgehog. Neuron. 1999; 22:103–114. [PubMed: 10027293]

Wei J, Zhao AZ, Chan GC, Baker LP, Impey S, Beavo JA, Storm DR. Phosphorylation and inhibition of olfactory adenylyl cyclase by CaM kinase II in neurons: a mechanism for attenuation of olfactory signals. Neuron. 1998; 21:495–504. [PubMed: 9768837]

Westrum LE, Blackstad TW. An electron microscopic study of the stratum radiatum of the rat hippocampus (regio superior, CA 1) with particular emphasis on synaptology. J Comp Neurol. 1962; 119:281–309. [PubMed: 14000149]

Yao PJ, Petralia RS, Bushlin I, Wang Y, Furukawa K. Synaptic distribution of the endocytic accessory proteins AP180 and CALM. J Comp Neurol. 2005; 481:58–69. [PubMed: 15558718]

Zerlin M, Levison SW, Goldman JE. Early patterns of migration, morphogenesis, and intermediate filament expression of subventricular zone cells in the postnatal rat forebrain. J Neurosci. 1995; 15:7238–7249. [PubMed: 7472478]

Zheng X, Mann RK, Sever N, Beachy PA. Genetic and biochemical definition of the Hedgehog receptor. Genes Dev. 2010; 24:57–71. [PubMed: 20048000]

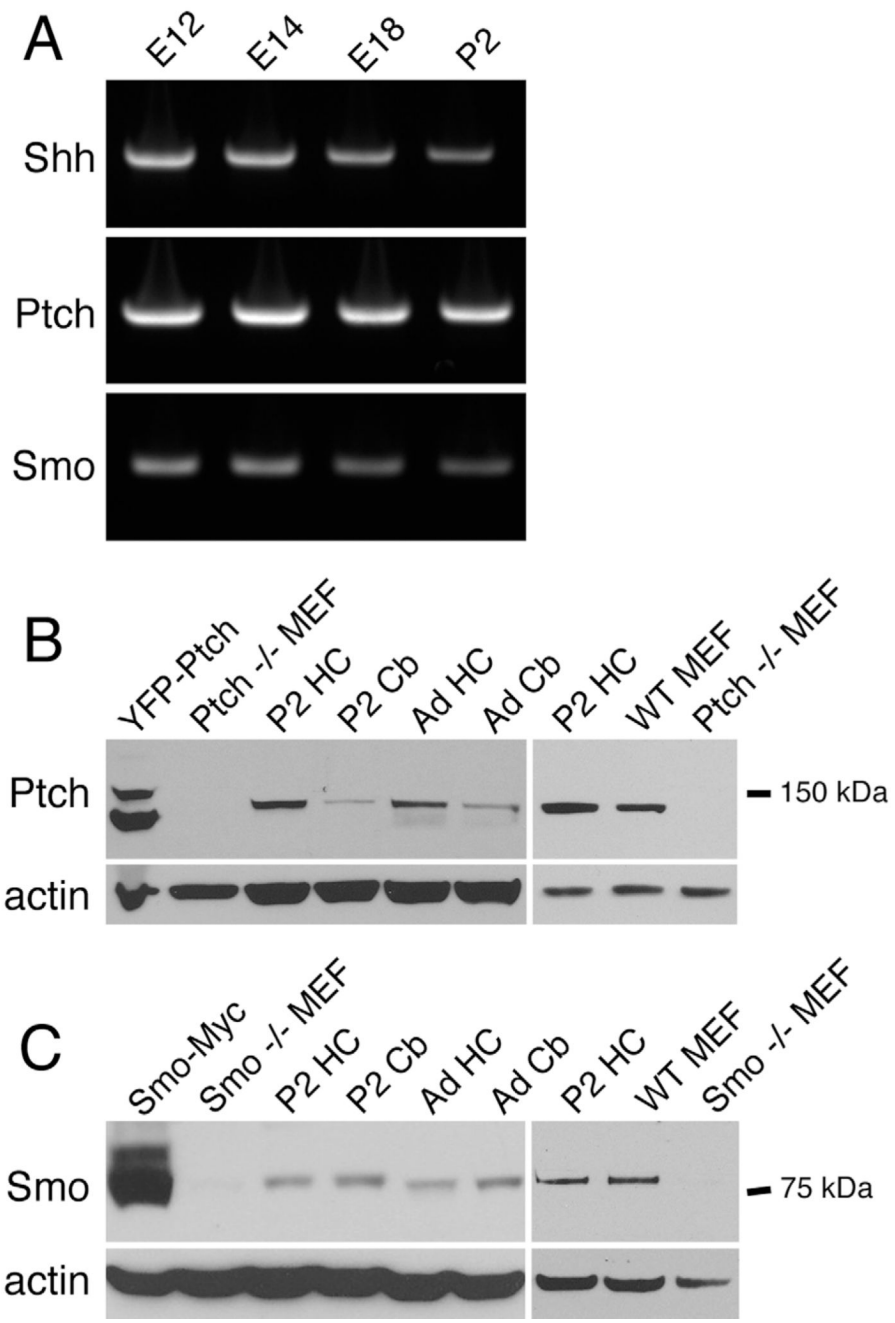

Figure 1.

Ptch and Smo are expressed in the developing and mature brains. **A:** RT-PCR analysis shows the expression of mRNAs encoding Shh, Ptch, and Smo in the brains of rats at the indicated ages. E, embryonic; P, postnatal. **B:** An antibody to Ptch detects a band at ~130 kDa. The band is not detected in Ptch−/− MEFs but is detected in rat brain tissues and wild-type MEFs. In lysates of HEK293 cells expressing a YFP-Ptch cDNA construct, the antibody detected two bands. The upper protein band may reflect the YFP-Ptch fusion protein, whereas the lower band may be partially degraded YFP-Ptch. HC, hippocampus; Cb, cerebellum; Ad, adult (postnatal day 35). **C:** An antibody to Smo detects a band at ~80

kDa. The band is not detected in Smo−/− MEFs, but is detected in rat brains and wild-type MEFs. No image adjustments were performed on the blots.

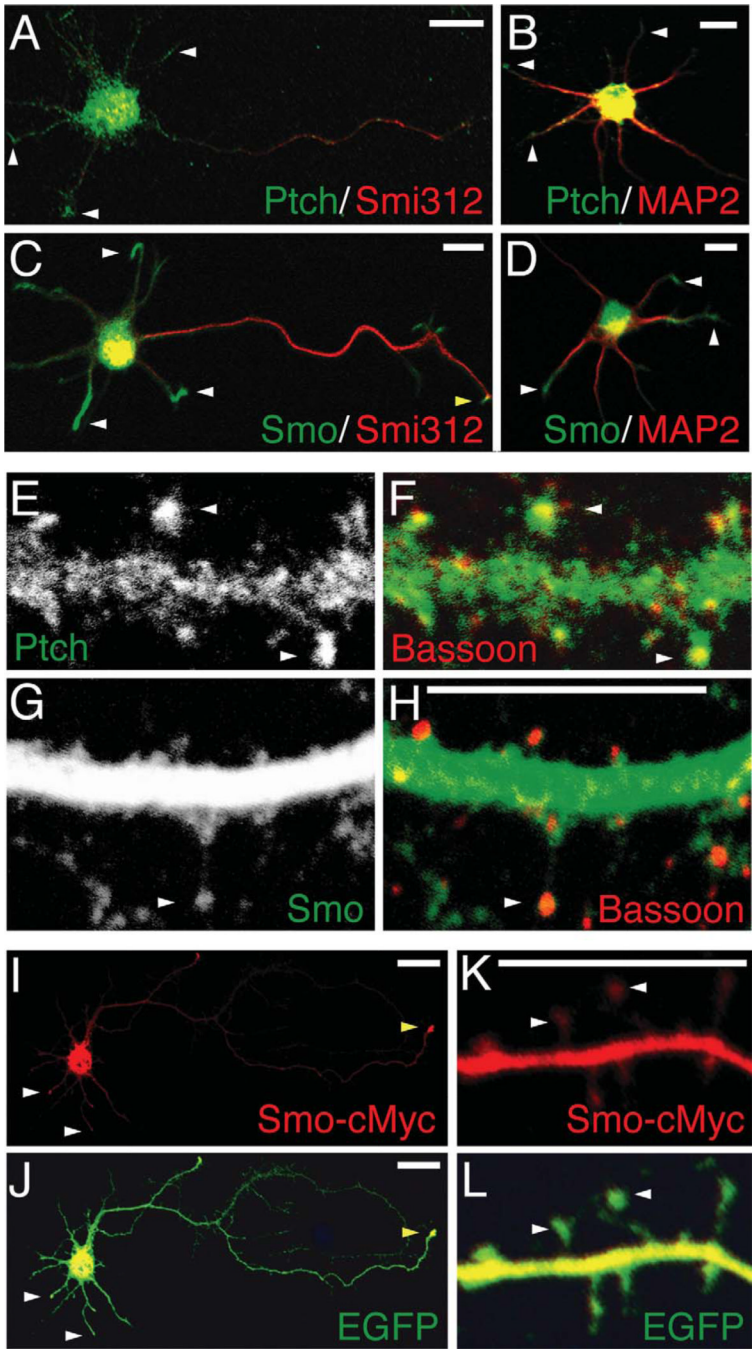

Figure 2.

Distribution of Ptch and Smo in cultured hippocampal neurons. **A–D:** Immunofluorescence labeling of Ptch and Smo in young hippocampal neurons (2 div). Double labeling of Ptch (green) with the axonal marker Smi312 (red) or the dendritic marker MAP2 (red) shows that, in addition to the soma, Ptch is detected in the tips of dendrites (white arrowheads). Double labeling of Smo (green) with Smi312 or MAP2 shows bright Smo labeling in dendritic tips (white arrowheads) and faint Smo labeling in axonal tips (yellow arrowhead). **E–H:** Immunofluorescence labeling of Ptch and Smo in mature hippocampal neurons (20 div). White arrowheads in E and F indicate Ptch labeling in spine heads, paired with the

presynaptic marker bassoon (red). G and H show substantially more Smo labeling in dendrites than in spine heads (arrowhead). **I,J:** A cultured hippocampal neuron (2 div) co-expressing Smo-cMyc and EGFP. An antibody to cMyc (red) reveals Smo-cMyc in dendritic (white arrowheads) and axonal (yellow arrowhead) tips. **K,L:** A cultured hippocampal neuron (20 div) expressing Smo-cMyc. The ectopically expressed Smo-cMyc is more intense in dendrites and weaker, but not absent, in spine heads (arrowheads). Scale bar = 10 mm in A–D; 5 mm in H (applies to E–H), and K (applies to K,L); 20 mm in I,J.

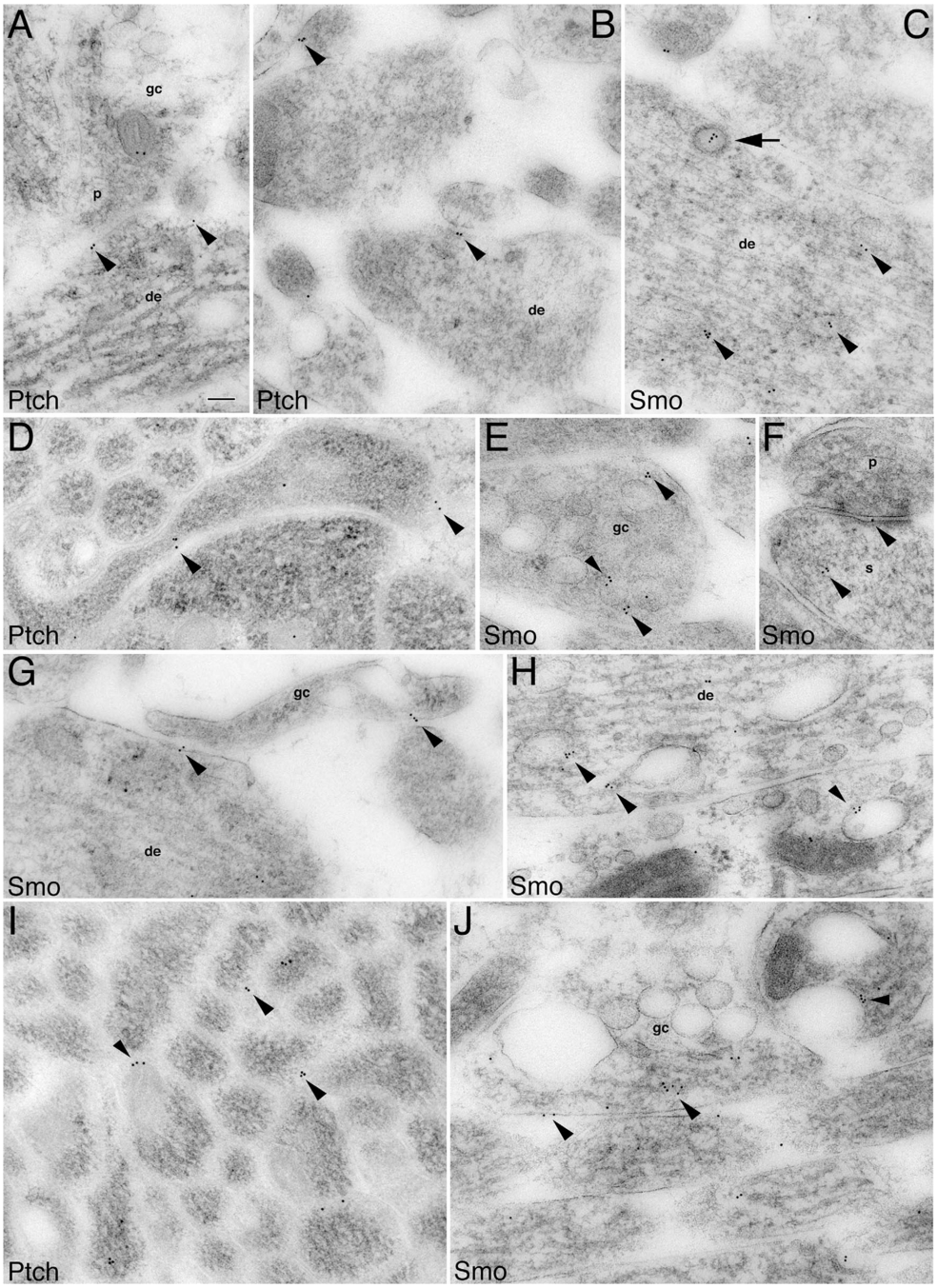

Figure 3.

Subcellular localization of Ptch and Smo in immature processes and growth cones of developing hippocampal neurons. Immunogold labeling for Ptch and Smo in P2 hippocampus CA1 stratum radiatum (A,F,H), and the developing white matter plus stratum oriens dorsal to the CA1 stratum pyramidale (B–E,G,I,J). *Ptch labeling:* **A:** An axonal growth cone (gc) forms an immature presynaptic terminal (p) contacting a young dendrite (de) where Ptch labeling is located at the membrane of the contact points (arrowheads). **B:** Additional examples of Ptch labeling situated at the contacts (arrowheads). **D:** An unidentified growing process in which Ptch labeling is at contacts with adjacent processes.

I: Ptch labeling located in between axons of a large axon bundle (transverse view). *Smo labeling:* **C:** A presumptive newly generated neuron with abundant microtubules and neurofilaments shows Smo labeling, which associates with cytoplasmic organelles (arrowheads) including a clathrin-coated vesicle (arrow). **E:** Smo labeling is found near or on endosomes (arrowheads) that are highly abundant in growth cones. **F:** Smo labeling in the spine(s) of a nascent synapse. **G:** Smo labeling is seen at the contacts of a growth cone with a young dendrite and an unidentified process. **H:** Smo labeling on endosomes of young dendrites. **J:** Longitudinal view of axons: one of these axons is expanded into a large growth cone. Smo labeling (arrowheads) is seen at the plasma membrane and near or on endosomes. Scale bar = 100 nm in A (applies to A–J).

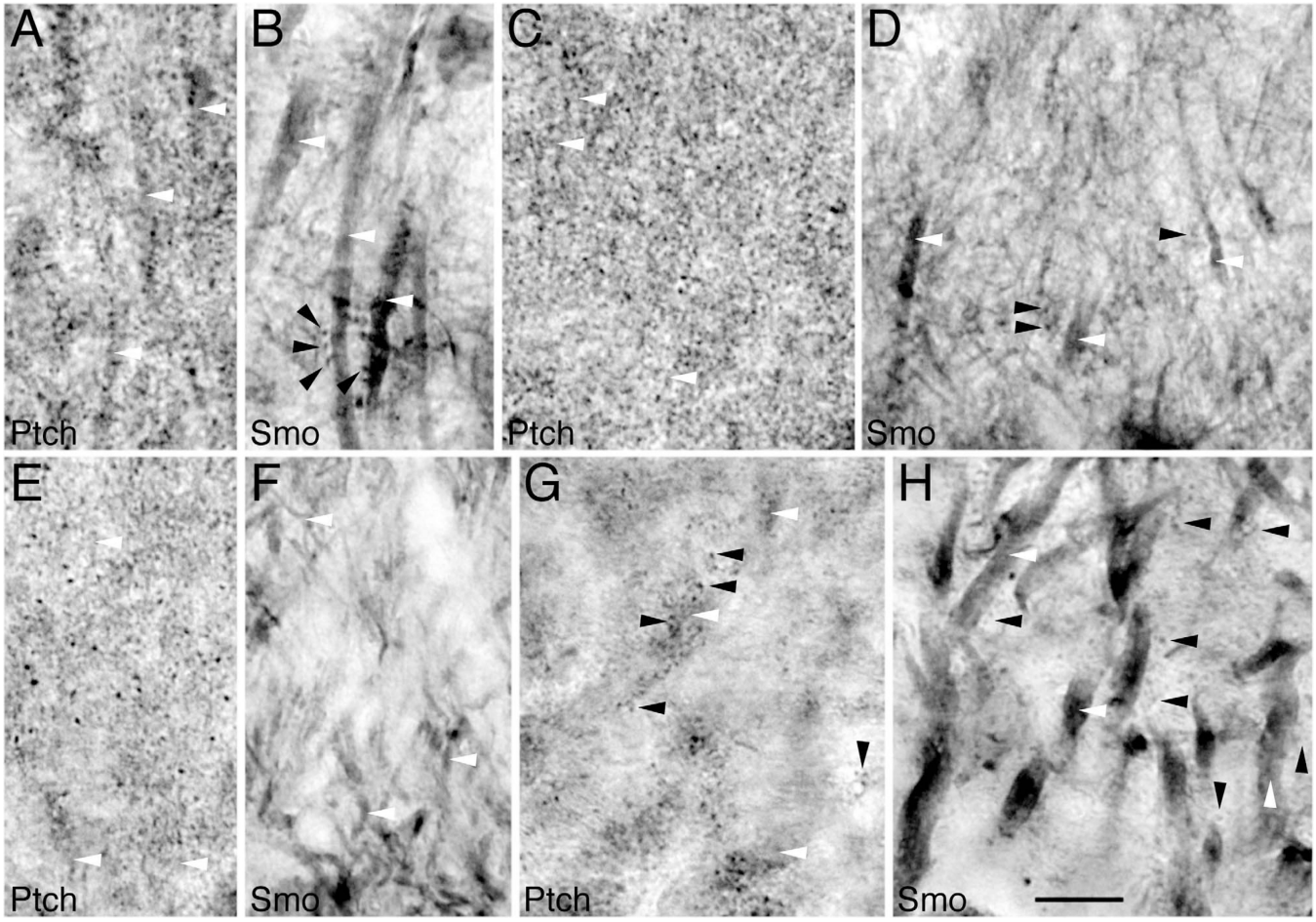

Figure 4.
Cellular distribution of Ptch and Smo in the hippocampus of adult rats using immunoperoxidase/DAB light microscopy. **A,B:** The CA1 stratum radiatum. **C,D:** The CA1 stratum oriens. **E,F:** The molecular layer of the dentate gyrus. **G,H:** The CA3 stratum lucidum. In all regions, intensely labeled Ptch puncta (black arrowheads) surround lightly labeled dendrites (white arrowheads). In contrast, Smo labels dendrites (white arrowheads) more intensely than puncta (black arrowheads). Scale bar = 10 mm in H (applies to a–H).

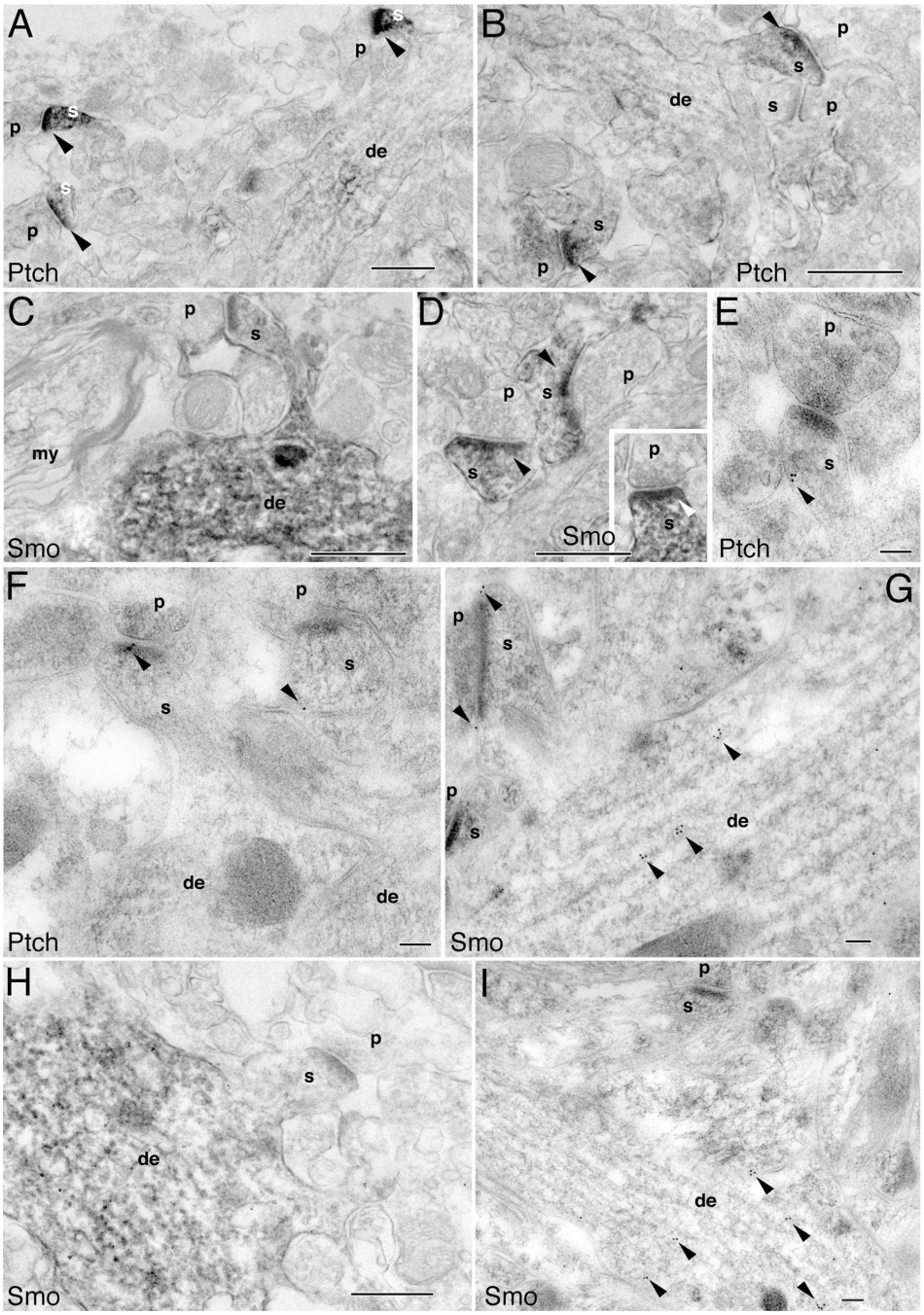

Figure 5.

Postsynaptic localization of Ptch and Smo in mature hippocampal neurons. Ptch and Smo labeling in the CA1 stratum radiatum (A,B,E,F,H,I), CA3 stratum radiatum (C,G), and the CA1 stratum oriens (D) of the adult hippocampus. A–D,H are immunoperoxidase/DAB and E–G,I are immunogold labeling. **A,B:** Intense Ptch labeling (arrowheads) in spines (s), with little or no labeling in dendrites (de) or the presynaptic terminals (p). **C:** Example of a Smo distribution pattern whereby Smo labeling is prominent in dendrites. Also note that the presynaptic terminal (p) and a nearby myelinated axon (my) do not have Smo labeling. **D,inset:** Examples of Smo-containing spines synapse with Smo-absent presynaptic

terminals. **E,F:** Ptch immunogold particles within spines (arrowheads). **G:** Smo immunogold particles in the spine as well as in the dendrite (arrowheads). **H:** Another example of positive Smo immunoperoxidase labeling in a dendrite. **I:** Another example of Smo immunogold labeling (arrowheads) in a dendrite. Scale bar = 500 nm in A–D,H; 100 nm in E–G,I.

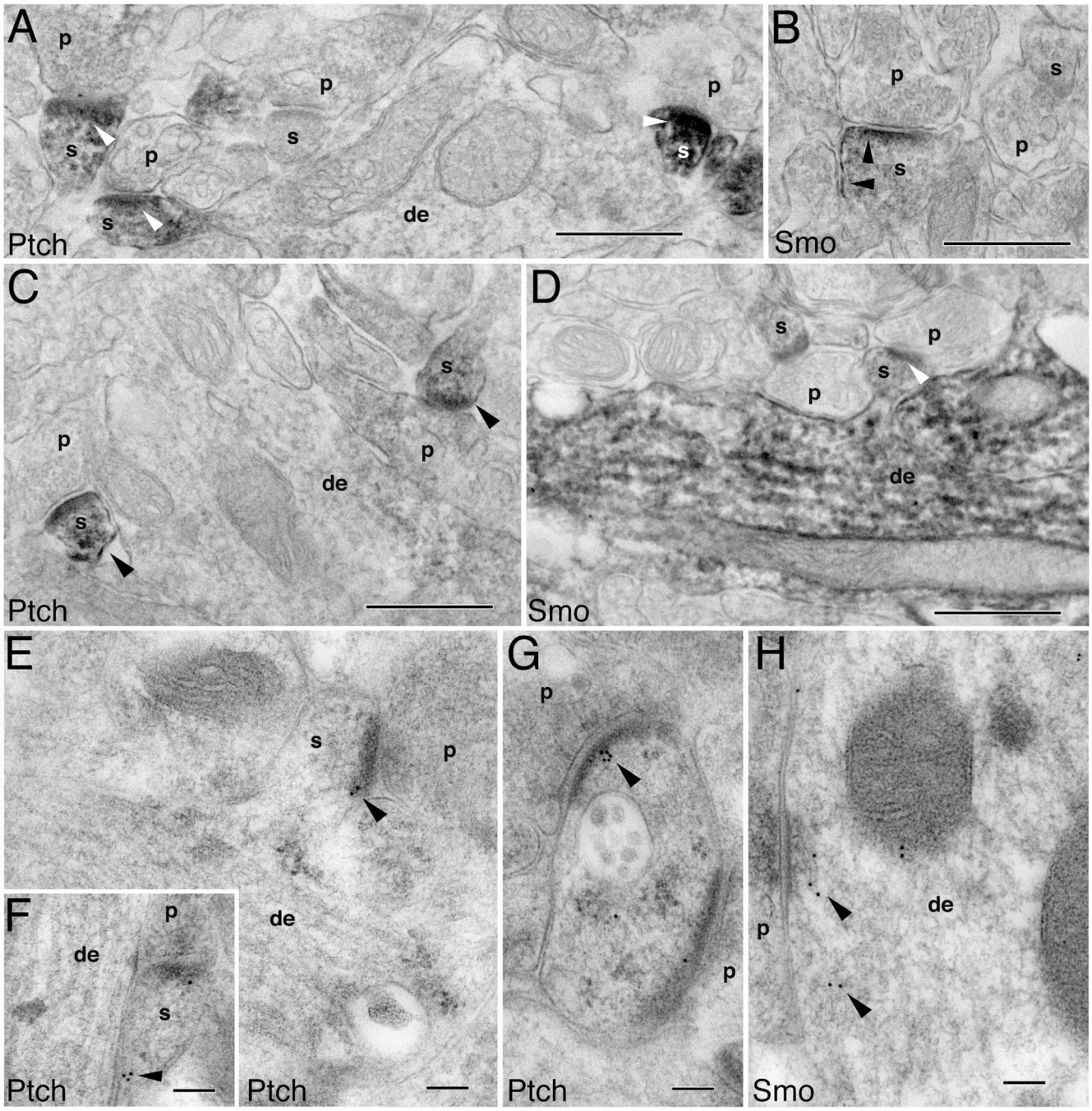

Figure 6.

Postsynaptic distribution of Ptch and Smo in the molecular layer of the dentate gyrus. A–D are immunoperoxidase/DAB labeling and E–H are immunogold labeling. **A,C:** Ptch labeling (arrowheads) is high in spines (s) and low in dendrites (de). **B,D:** Smo labeling is found in spines (arrowheads in B) but is prominent in dendrites (D). **E–G:** Examples of Ptch immunogold labeling in spines (arrowheads). **H:** Example of Smo immunogold labeling in a dendrite (arrowheads). Scale bar = 500 nm in A–D; 100 nm in E–H.

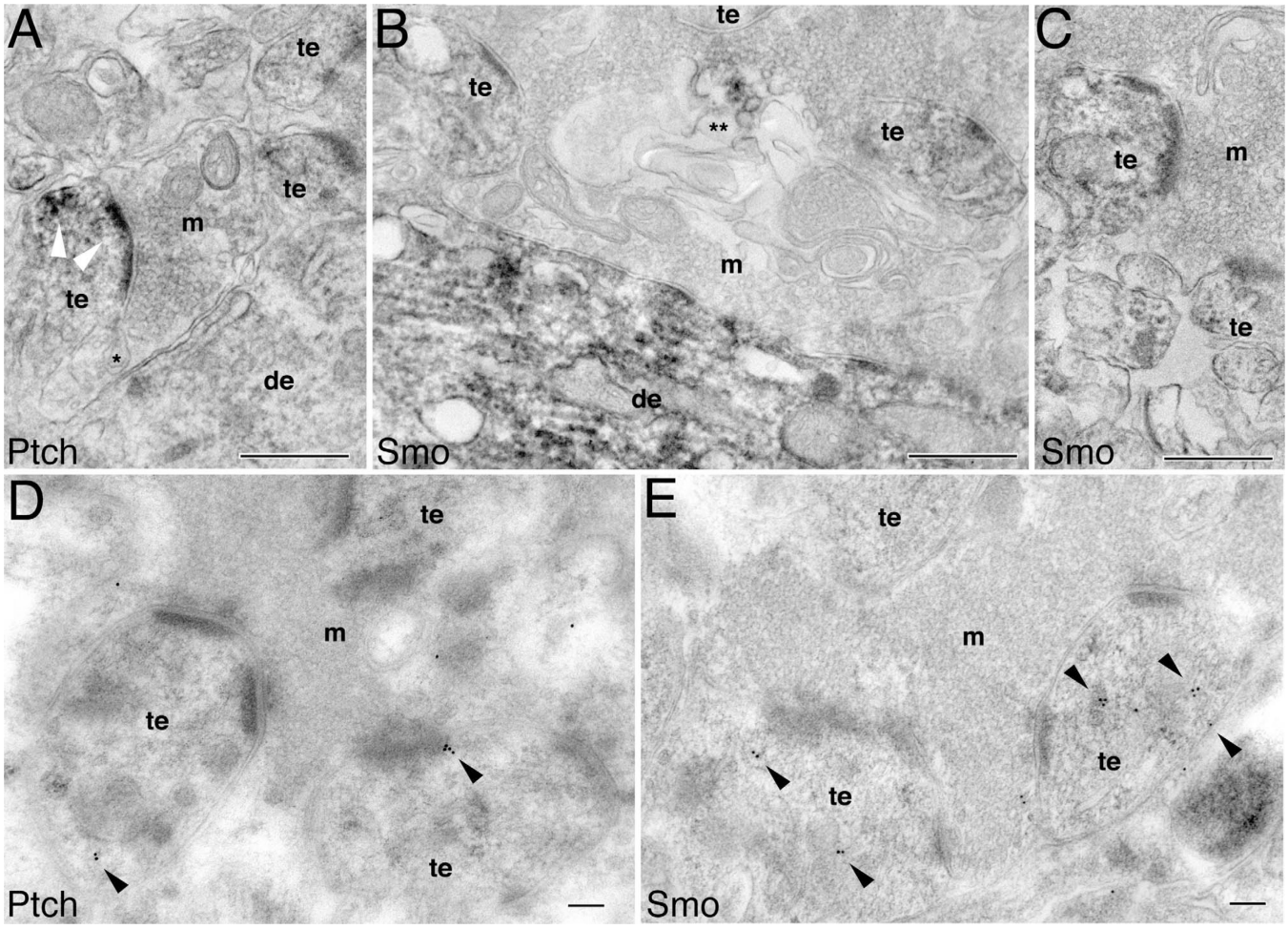

Figure 7.

Postsynaptic distribution of Ptch and Smo in the CA3 mossy terminal area (stratum lucidum) of the adult hippocampus. A–C are immunoperoxidase/DAB labeling and D,E are immunogold labeling. **A:** Presence of Ptch labeling (white arrowheads) in the postsynaptic thorny excrescences (te), and absence of the labeling in the dendrite (de) and mossy terminal (m). * marks a spinule. **B:** Intense Smo labeling in dendrites and moderate labeling in thorny excrescences. ** marks a Smo-labeled autophagosome-like structure. **C:** Another example of Smo-labeled thorny excrescences surrounded by an unlabeled mossy terminal. **D:** Ptch immunogold (arrowheads) in thorny excrescences. **E:** Smo immunogold (arrowheads) mainly associated with intracellular organelles in thorny excrescences. Scale bar = 500 nm in A–C; 100 nm in D,E.

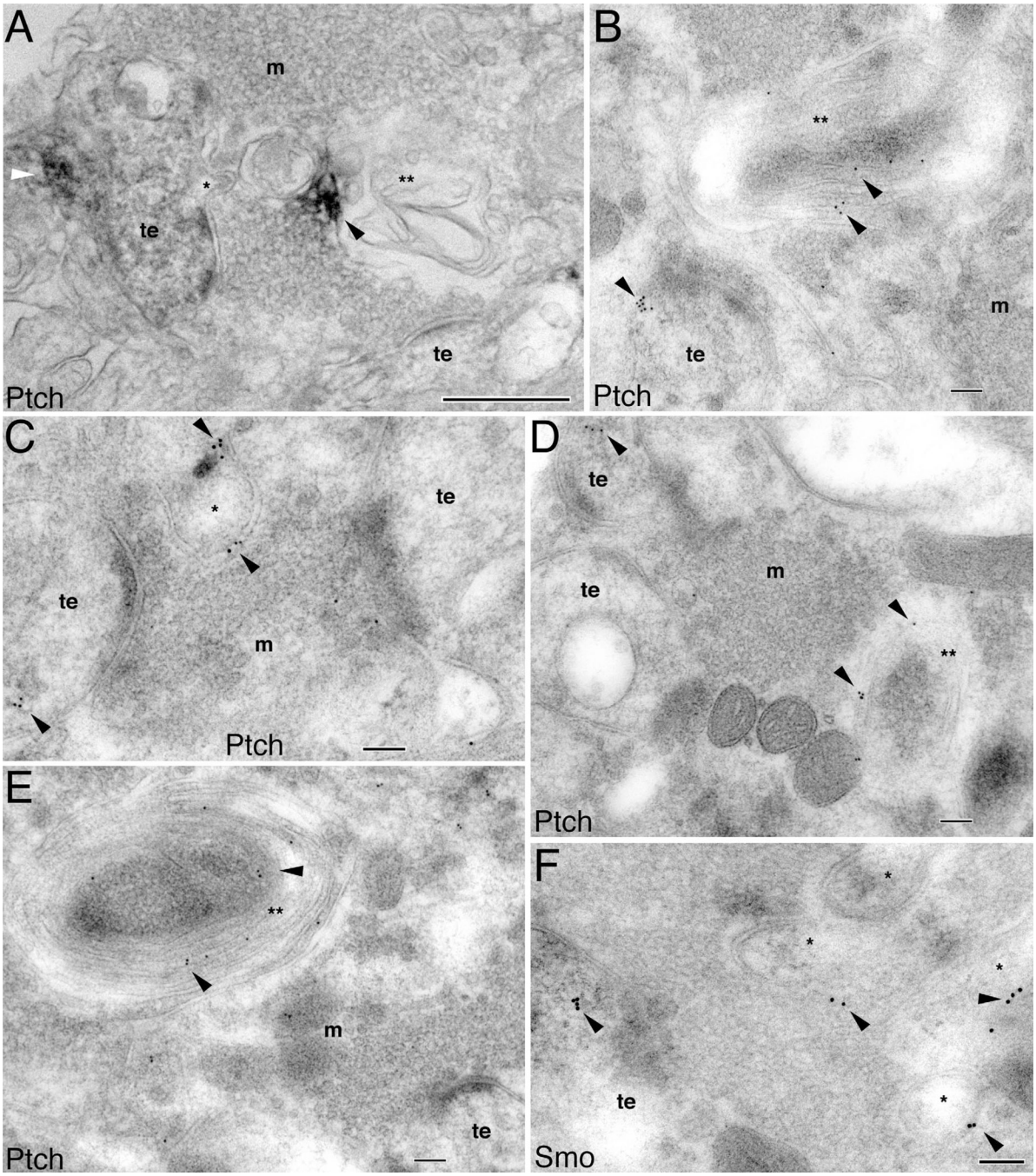

Figure 8.

Association of Ptch and Smo with synaptic spinules and autophagosomes in the CA3 mossy terminal area of the adult hippocampus. A is immunoperoxidase/DAB labeling and B–F are immunogold labeling. **A:** A Ptch-labeled thorny excrescence (te) with a spinule (*) that is oriented toward the surrounding mossy terminal (m); Ptch labeling (white arrowhead) is not within the spinule. Ptch labeling (black arrowhead) is also seen in a nearby irregular shaped autophagosome (**). Note the near contiguous sequence of three structures in the mossy terminal, from the spinule, to a larger spinule-like structure, to the even larger, labeled autophagosome. **B:** Ptch immunogold labeling (arrowheads) in a thorny excrescence (te) and

in a nearby large autophagosome (**). **C,D:** Ptch immunogold (arrowheads) within the thorny excrescences (te), a relatively large spinule (*), and autophagosome (**). **E:** Ptch immunogold bonded to the plasma membranes of autophagosome whorls (**). **F:** Examples of Smo immunogold in the large spinules (*) in addition to the thorny excrescence (te). Scale bar = 500 nm in A; 100 nm in B–F.

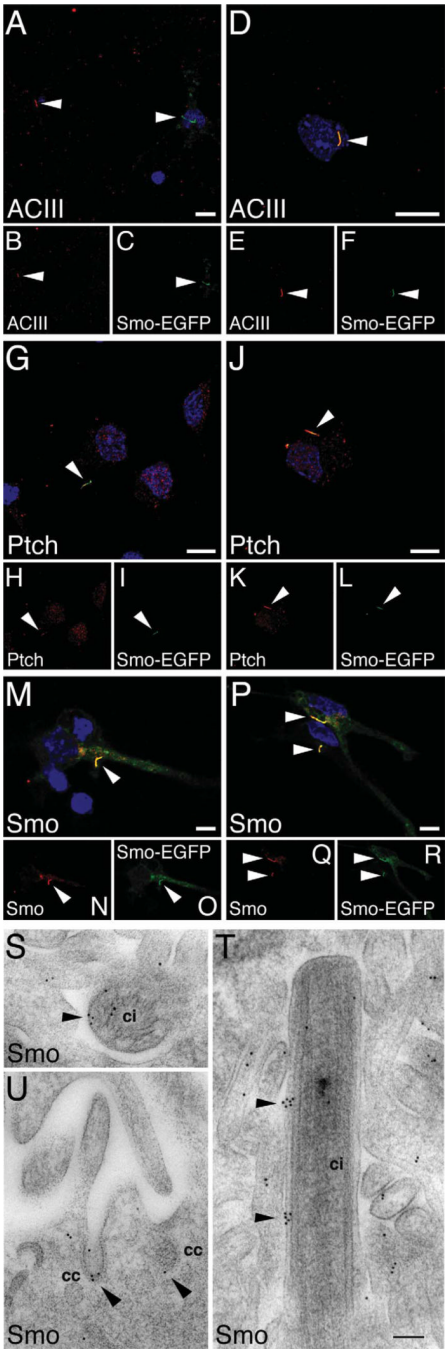

Figure 9.

The distribution of Ptch and Smo in relation to the primary cilium. Hippocampal neurons (2 div) were transfected with Smo-EGFP, and, 2 days later, labeled with antibody as indicated. A–F are examples of ACIII-labeled neurons. **A–C:** ACIII is absent in a Smo-EGFP-expressing cilium. **D,E:** ACIII is present in a Smo- EGFP-cilum. **G–L:** Examples of Ptch-labeled neurons. **M–R:** Examples of Smo-labeled neurons. S–U: Immunogold labeling for Smo in the choroid plexus, rostral to the hippocampus of P2 rat (sagittal sections). S**:** Cross-section view of a primary cilium (ci), where Smo immunogold labeling (arrowheads) is seen on its surface and within. **T:** Longitude view of a primary cilium (ci). In addition to the

surrounding microvilli, Smo immunolabeling is mostly on the surface of the primary cilium (arrowheads). **U:** Smo immunogold labeling (arrowheads) in clathrin-coated vesicles (cc) that are located at the base of microvilli. Scale bar = 10 mm in A (applies to A–C), D (applies to D–F), G (applies to G–I), J (applies to J–L), M (applies to M–O), and P (applies to P–R); 100 nm in T (applies to S–U).

TABLE 1.

Antibodies Used in This Study

Antigen	Immunogen	Host isotype	Working dilution	Source, cat. no.
Ptch	N-terminal peptide of human Ptch (amino acids 1–40)	Rabbit serum Rabbit serum	1:200 for blots 1:100 for labeling	Abcam, ab53715
Smo	Peptide of human Smo (amino acids 772–787)		1:200 for blots 1:100 for labeling	Abcam, ab38686
β-Actin	N-terminal peptide of the β-isoform of actin (DDDIAALVIDNGSGK)	Mouse IgG_1	1:5,000	Sigma (clone AC-15), A5441
Neurofilament	The nonphosphorylated neurofilament H in homogenized rat brain	Mouse	1:1,000	Covance, SMI-312R
(Smi312)		IgG_1		
MAP2	A peptide shared by all isoforms of MAP2 (KNVRSKVGSTENIKHQPGGGRAK)	Mouse IgG_1	1:2,500	Sigma (clone HM-2), M9942
Bassoon	A peptide of rat bassoon (amino acids 738–1,035)	mouse IgG_{2a}	1:100	Stressgen, VAM-PS003
Adenylyl cyclase III (ACIII)	C-terminal peptide of mouse ACIII(PAAFPNGSSVTLPHQVVDNP)	Rabbit serum	1:500	Santa Cruz, Sc-588